ORIGINAL REPORT

High-content Image-based Drug Testing of Patients' Primary Fibroblasts Reveals Potential New Treatment Options for Localized Scleroderma

Katariina MÄHÖNEN[1], Isabel MOGOLLON[2], Antti HASSINEN[2], Minttu POLSO[2], Katja VÄLIMÄKI[2], Swapnil POTDAR[2], Al-Amin CHOWDHURY[1], Annamari RANKI[1†], Jani SAARELA[2], Vilja PIETIÄINEN[2#] and Jaana PANELIUS[1#]

[1]Department of Dermatology and Allergology, University of Helsinki and Helsinki University Hospital, Helsinki, Finland, and [2]Institute for Molecular Medicine Finland – FIMM, Helsinki Institute for Life Sciences – HiLIFE, University of Helsinki, Helsinki, Finland

[†]Author deceased. [#]These authors contributed equally.

Localized scleroderma is a rare autoimmune disease characterized by progressive fibrosis of the skin and its underlying structures, causing loss of normal tissue structure and function. Myofibroblasts, differentiated from fibroblasts by high expression of α-smooth muscle actin, play a key role in the pathogenesis with continuous production of collagen and other extracellular matrix components. Transforming growth factor β promotes myofibroblast transformation and is central to the pathogenesis of fibrotic diseases. Targeted therapies for skin fibrosis are lacking, and current treatment consisting of topical steroids and immunosuppressive drugs often has limited efficacy. In this study, testing was performed with 78 drugs on lesional localized scleroderma fibroblasts to find potential new therapies, with α-smooth muscle actin and collagen-1 expression as markers for antifibrotic effect. Several drugs belonging to inhibitors of tyrosine kinase, phosphoinositide-3 kinase, and transforming growth factor β receptor were found to have an antifibrotic effect in localized scleroderma fibroblasts. Along with increased expression of transforming growth factor β1, Smad3, and AKT found in lesional localized scleroderma skin, these results confirm transforming growth factor β pathway as a treatment target. Additionally, androgen receptor antagonists showed potential antifibrotic effects, co-aligning with an increased expression of androgen receptor in localized scleroderma skin.

Key words: localized scleroderma; high throughput screening assay; myofibroblasts; transforming growth factor beta; antifibrotic agents.

Submitted Feb 25, 2025. Accepted after revision Jul 7, 2025

Published Aug 3, 2025. DOI: 10.2340/actadv.v105.43088

Acta Derm Venereol 2025; 105: adv43088.

Corr: Katariina Mähönen, Department of Dermatology and Allergology, Skin and Allergy Hospital, P.O. Box 160, 00029 HUS Helsinki, Finland. E-mail: katariina.mahonen@hus.fi

SIGNIFICANCE

Localized scleroderma is an autoimmune connective tissue disease, where chronic inflammation and abnormal activation of myofibroblasts leads to permanent skin fibrosis. Currently there are no specific therapies targeting fibrosis. In this study, we aimed to find potential new antifibrotic treatments for localized scleroderma, using image-based drug screening assay for fibroblasts isolated from the skin of localized scleroderma patients. We found several drug groups with antifibrotic effects, among them inhibitors of tyrosine kinase, transforming growth factor β receptor, and phosphoinositide-3 kinase, as well as androgen receptor antagonists. Our study suggests new treatment options for localized scleroderma.

Localized scleroderma (LS) is a rare autoimmune disease characterized by fibrosis of the skin and its underlying tissues (1). The pathogenesis of LS has similarities to systemic sclerosis (SSc), but the diseases are separate entities, and LS does not progress to systemic disease (2, 3). Although LS is not life-threatening, in deep subtypes it can lead to disfigurement and joint contractures and cause ophthalmological and neurological problems when located in the head (1, 2).

The fibroblast plays a key role in the pathogenesis of LS. In genetically predisposed persons, an initiating factor (i.e., trauma, radiation, infections) leads to vascular injury, starting an inflammatory process (1, 3, 4). Several cytokines and growth factors promote fibroblast transformation into active myofibroblasts, characterized by the expression of α-smooth muscle actin (α-SMA) (5, 6). Myofibroblasts are contractile cells able to secrete large amounts of extracellular matrix (ECM) components including collagen-1 and accumulate at the site of tissue injury in wound-healing response (6, 7). Myofibroblasts normally undergo apoptosis after they are no longer needed, but in pathological fibrotic conditions they remain active at the site (5–7). Myofibroblasts produce profibrotic cytokines such as interleukin -1, -6 and -8, and growth factors, such as vascular endothelial growth factor (VEGF) and transforming growth factor β (TGF-β) (7). TGF-β stimulates further myofibroblast formation leading to a self-perpetuating cycle, promotes fibrinogenic phenotype of immune and vascular cells, and through SMAD-signalling induces the synthesis of ECM components (8, 9). Continuous myofibroblast activation and TGF-β signalling leads to accumulation of ECM components, fibrosis, and loss of normal tissue structure.

LS is currently treated with topical steroids and UVA phototherapy (10). In the case of widespread disease or deep tissue involvement, methotrexate and systemic glucocorticoids are the first-line systemic treatments (2, 10). Methotrexate has a wide immunosuppressive effect, but it does not specifically target fibrosis (11). Nintedanib, a tyrosine-kinase (TK) inhibitor, and tocilizumab, an interleukin-6 monoclonal antibody, both with antifibrotic properties and FDA approved for treatment of SSc interstitial lung disease, did not have a statistically significant effect on skin fibrosis (12). New treatment options for skin fibrosis are warranted (13).

High throughput (HT) screening allows a multitude of drugs to be tested simultaneously on target cells to search for potential new treatments (14). Cancer cell lines and patient-derived cancer cells are commonly used for HT drug screening, which may lead to new targeted treatment options and clinical trials. In the context of SSc, it has been proposed that organoid models and patient-derived cells could be utilized for drug screening, and a personalized *in vitro* drug testing model using real-time quantitative PCR has been suggested (15, 16). One HT-drug screening study has been conducted using fibroblasts, which were differentiated from induced pluripotent stem cells generated from SSc patient peripheral blood mononuclear cells, finding that raloxifene reduced fibroblast proliferation and ECM production (17).

In this study, we used to our knowledge for the first time lesional LS skin fibroblasts to perform drug screening to find potential new drugs to target fibrosis. We cultured fibroblasts isolated from lesional skin of 3 LS patients and performed drug screening with 78 drugs, including 15 investigational agents. We used high content (HC) confocal imaging to assess the antifibrotic effect of the drugs as determined by the reduction in expression of α-SMA, a marker for myofibroblasts, and collagen-1.

MATERIALS AND METHODS

Study participants and sample collection

LS patients were recruited from the Skin and Allergy Hospital's dermatological outpatient clinic. Inclusion criteria were age > 18 years, diagnosis of LS, and active disease (new or growing lesions within the last year). A surgical excision was performed on lesional LS skin. From 3 female patients with plaque morphea, part of the biopsy was processed for fibroblast culture and another part formalin-fixed and paraffin-embedded (FFPE) for immunohistochemistry (IHC). One of the patients had undergone UVA phototherapy (3 years prior) and used methotrexate (2 years prior to participation). For IHC, an additional 7 LS patient skin samples were included (**Table I**). Participation was voluntary, and all participants signed an informed consent. Control skin samples were obtained from the department's dermatosurgical unit from patients undergoing skin graft procedures. Control individuals were not diagnosed with LS or SSc.

Fibroblast isolation and culture

Biopsies were washed with phosphate-buffered saline (PBS) and subcutaneous adipose tissue was mechanically removed. Fibroblasts were isolated with a human whole skin dissociation kit (Miltenyi Biotec, Bergisch Gladbach, Germany) according to the manufacturer's instructions, using gentle MACS dissociator (Miltenyi Biotec). After the dissociation protocol, the centrifuged fibroblasts were resuspended with culture medium and seeded on non-coated plastic cell culture flasks. Cells were maintained in high glucose-DMEM (Gibco, Thermo Fisher Scientific, MA, USA) supplemented with heat-inactivated 10% fetal bovine serum (Gibco, Thermo Fisher Scientific), 1% glutamax (Gibco, Thermo Fisher Scientific), and 1% penicillin-streptomycin (Gibco, Thermo Fisher Scientific). After reaching 70% confluency, cells were trypsinized with 1x trypsin EDTA (Gibco, Thermo Fisher Scientific), and centrifuged at 1,000 rpm. The pellet was resuspended in culture medium and seeded on culture flasks at 1:3 ratio. Fibroblasts were cultured until passage 2 or 3, to avoid changes in cell phenotype.

Drug screening

Seventy-eight drugs were included for screening, each in 5 different concentrations (Table SI). The compounds

Table I. Characteristics of the study participants

Patient	Sex	Age, years	Clinical phenotype	Systemic treatment at the time of sampling	Previous treatment	Disease duration, years	Biopsy site
1	Female	33	Plaque	–	–	19	Left arm
2	Female	65	Plaque	–	–	5	Abdomen
3	Female	35	Plaque	–	Phototherapy (UVA), MTX	7	Abdomen
4	Male	58	Plaque	–	Phototherapy (UVA)	3	Left flank
5	Female	66	Plaque	–	Phototherapy (UVA), cyclosporine	5	Abdomen
6	Female	38	Plaque	–	Phototherapy (UVA)	12	Left flank
7	Male	38	Generalized	–	Phototherapy (UVA)	4	Upper back
8	Female	27	Plaque	MTX	–	0	Right thigh
9	Female	32	Linear	MTX	–	16	Left shoulder
10	Female	69	Plaque	–	Phototherapy (UVA)	1	Right armpit

Fibroblasts were isolated from the lesional skin of patients 1–3. MTX: methotrexate.

were dispensed to tissue-culture treated 384-well assay plates (Cell Carrier ultra, PerkinElmer, Waltham, MA, USA) using acoustic dispensing (Echo 650, Beckman-Coulter, Brea, CA, USA). 0.1% DMSO was used as negative and 100 000 nM benzethonium chloride as positive control. After trypsinization and cell counting, 500 cells/well were seeded on drug plates using BioTek Multiflo FX RAD dispenser (Agilent, Santa Clara, CA, USA) in 25 µl of culture medium and incubated for 72 h at 5% CO2 at 37ºC, after which fixed for 15 min at room temperature (RT) in 4% formaldehyde (Sigma-Aldrich, St Louis, MO, USA). Following fixation, cells were washed and stored in PBS. Washing, liquid dispensing, and aspiration were performed using the BioTek EL406 Washer Dispenser (Agilent).

Cells were permeabilized in 0.3% Triton X-100 in PBS for 10 min at RT and blocked in PBS containing 3% bovine serum albumin (BSA, Biowest, Nuaillé, France) for 60 min at RT. After washing, the primary antibodies (anti-collagen-1, AB745, 1:100, Millipore, Bedford, MA, USA and anti-α-SMA, ab7817, 1:200, Abcam, Cambridge,UK) were added using Certus FLEX 0.3 liquid handling system (Gyger, Gwatt, Switzerland) and cells incubated for 1 h at 37°C. After washing with PBS, Alexa Fluor-conjugated secondary antibodies (goat anti-mouse 488, A11001, 1:1000, Invitrogen, Waltham, MA, USA and goat anti-rabbit 568, A11011, 1:1000, Invitrogen), along with Hoechst 33242 (H1399, 1:10000, Life Technologies, Carlsbad, CA, USA) and HCS Cell Mask Far Red (32721, 1:40000, Thermo Fisher Scientific) were added. Collagen-1 was stained green (AF488) and α-SMA orange (AF568). Fibroblasts from patient 3 and control 3 were stained in an inverted manner (collagen-1 in orange and α-SMA in green) but displayed similar patterns of expression (Fig. S1). The cells were incubated for 1 h at RT, after which they were washed and stored at +4°C.

High content imaging and analysis

HC imaging was performed with PerkinElmer Opera Phenix spinning disk confocal microscope (High Content Imaging and Analysis Unit, FIMM, HiLIFE, University of Helsinki, Finland) using a 20x water immersion objective (NA 1.0, working distance 1.7 mm, depth of focus 1.8 µm) with 4 excitation lasers (405 nm with emission band-pass filter 435/480; ex 488, em 500/550; ex 561, em 570/630, and ex 640, em 650/760). Nine fields of view with 5% overlap were imaged per well using 3 predetermined Z focus planes with laser-based autofocusing. The images were captured with 2 Andor Zyla sCMOS cameras (16-bit, field of view 650 x 650 µm2, effective xy resolution 0.66 µm). Z-stacks were analysed from a maximum projection using the Biology Image Analysis Software (BIAS) (Single-Cell Technologies, Szeged, Hungary) for primary image processing, segmentation, and extraction of intensity value features from collagen-1 and α-SMA channels. Image stacks were projected to 2D images using maximum intensity projection. Non-uniform illumination was corrected using the CIDRE method. Intensity features for collagen-1 and α-SMA were exported into .csv files and quantified using Python v3 (https://www.python.org/download/releases/3.0/). Drug hits were identified based on negative Spearman correlation, which measures the strength and direction of the association between drug concentration and normalized intensity values. The number of α-SMA positive cells was annotated using a BIAS software machine-learning based module by 1 expert. Spearman correlations, α-SMA positive cell ratio, and total cell number were normalized with DMSO controls. Cell viability was measured by the number of total segmented cells detected with BIAS segmentation. Statistical significance of Spearman correlation coefficients was determined across all compounds, and Benjamini-Hochberg correction was applied to adjust for multiple testing.

Immunohistochemistry

IHC was performed at FIMM Digital Microscopy and Molecular Pathology Unit supported by HiLIFE and Biocenter Finland on FFPE tissue sections. After deparaffinization, antigen retrieval was performed using a PT Module (Thermo Fisher Scientific) with Tris-EDTA buffer (pH 9.0) for 20 min. Endogenous peroxidase activity was blocked by 0.9% hydrogen peroxide incubation for 15 min at RT, after which the sections were blocked with 10% goat serum for 15 min at RT. The primary antibodies were diluted in the blocking solution as follows: mouse anti-androgen receptor (AR, 441) antibody (1:100, Ab9474, Abcam), rabbit anti-phosphorylated AKT antibody (1:100, CST4060, Cell Signaling Technology, Danvers, MA, USA), rabbit anti-Smad3 (Ser 213) antibody (1:200, Orb34522, Biorbyt, Cambridge, UK) and rabbit anti-TGF-β1 antibody (1:200, LS-B1004, LSBio, Seattle WA, USA). Antibodies against AKT and AR were incubated overnight at 4°C, and against Smad3 and TGF-β1 for 1 h at RT. After washing with Tris-buffered saline containing 0.05% Tween-20, the sections were incubated with species-specific secondary antibody conjugates for 30 min at RT (BrightVision HRP-Rabbit and HRP-Mouse, Immunologica, Arnhem, The Netherlands). The bound antibodies were visualized 3,3′-diaminobenzidine (DAB). The sections were counterstained with haematoxylin, dehydrated, and mounted with a coverslip.

Microscopy was performed using a 3D HISTECH Pannoramic 250 Flash III digital slide scanner (https://www.3dhistech.com/scanners/pannoramic-250-flash-iii-dx/) with a 20x objective (NA 0.8). Image analysis was conducted using QuPath version 0.50 (https://github.com/qupath/qupath/releases), employing the Positive Cell Detection module to quantify marker

expression. User-defined thresholds were applied to classify cells as negative, weakly positive, moderately positive, or strongly positive. The percentage of positive cells and Histoscores (H-scores), which combines staining intensity and the positive cell percentage into a single quantitative value, were extracted for further analysis from epidermis and upper dermis. The exported data from QuPath annotation areas were further analysed in Jupyter Lab (https://jupyter.org/) using Python. Group-wise comparisons of H-scores and positive cell percentage were visualized using box plots, which included *p*-values derived from the Mann–Whitney *U* tests.

RESULTS

Patient-derived fibroblasts were obtained from 3 LS patients with active plaque morphea, the most common LS subtype. The characteristics of the study patients are presented in Table I and study pipeline in **Fig. 1**A (discussed in detail in Methods). LS fibroblasts, as well as control fibroblasts, were exposed to 78 drugs in 5 different concentrations for 72 h (Table SI). The antifibrotic effects of the drugs were studied by an HC imaging-based readout, i.e., fluorescence staining of α-SMA and collagen-1. The expression patterns of collagen-1 and α-SMA were analysed from HC confocal images (Fig. 1B). In LS fibroblasts, a decrease in α-SMA and collagen-1 expression was found to occur with 58 and 28 drugs, respectively (**Fig. 2**A). The antifibrotic drugs were defined by a decrease in the mean intensity of both α-SMA and collagen-1 with increasing drug concentrations calculated as Spearman correlation, negative correlation meaning a decrease in marker expression (Fig. 2A and Fig. 2B). Importantly, cell viability determined by the total number of nuclei in the drug-treated vs control (DMSO) cells was found to remain constant in the increasing concentrations of the top hit drugs, i.e., the drugs were not cytotoxic. In the LS fibroblasts, 20 drugs showed an antifibrotic effect (**Table II**). We also analysed the ratio of α-SMA positive cells (myofibroblasts) to total cell number, and most of the drugs with negative Spearman correlations also showed a decrease in the α-SMA/total cell ratio, indicating that the drug effect was specific to myofibroblast and resulted in myofibroblasts deactivating into fibroblasts (**Fig. 3**).

Of the drugs with antifibrotic effect, 50% belonged to TK, phosphoinositide-3 kinase (PI3K), or TGF-β receptor inhibitors. Among the other drug groups with the effect were Rho-kinase inhibitors, androgen receptor (AR) antagonists, retinoids (acitretin), thalidomide, and Janus kinase (JAK)-inhibitors (filgotinib, decernotinib). Of note is that methotrexate, which is currently used to treat severe LS, did not show significant effect on α-SMA or collagen-1 expression in either LS or control fibroblasts. Among glucocorticoids, methylprednisolone showed an antifibrotic effect in the fibroblasts of 1 scleroderma patient, while prednisolone or dexamethasone did not have an antifibrotic effect (see Fig. S1). In control fibroblasts, antifibrotic effect was found in only 9 drugs, 6 of them the same as in LS fibroblasts (see Fig. 2A, Table II).

To further investigate the activation of signalling pathways affected by drugs with antifibrotic effects, we performed immunohistochemistry with FFPE LS skin samples and control skin. We performed staining for phosphorylated AKT (a serine/threonine kinase, also known as protein kinase B), which is a downstream protein activated by PI3K (18). AKT was expressed in the keratinocytes in the basal epidermis in 6/10 scleroderma skin samples, with weak positivity found in only 1 control sample (**Fig. 4**). TGF-β1 was expressed in keratinocytes, especially in the basal layer, with mild to moderate expression in all scleroderma samples. TGF-β1 was expressed weakly also in control samples, but expression was stronger in LS samples, with a statistically significant difference in both percentage of positive cells and H-score ($p = 0.04$) (Fig.4). We also performed IHC with SMAD3, which is a downstream protein of TGF-β1 and phosphorylated by type I receptor kinases upon activation of the TGF-β receptor mediating the fibrinogenic actions of TGF-β (9). Moderate to strong SMAD3 expression was found in all LS samples in keratinocytes (especially basal layer) and inflammatory cells. Among the control samples, mild to moderate positivity was found in 3/4 samples, but the percentage of positive cells was significantly lower as compared with scleroderma samples ($p = 0.03$). AR was found to be expressed in all LS samples (moderate to strong expression) in keratinocytes and inflammatory cells. Among the control skin samples, 3 samples showed mild expression and 1 moderate, but the percentage of positive cells was significantly lower than in LS samples ($p = 0.02$) (Fig. 4).

DISCUSSION

Tyrosine-kinase -, epidermal growth factor - and PI3K inhibitors have antifibrotic properties according to the literature (19-22). The PI3K/AKT pathway is recognized as important for normal skin homeostasis and its pathological activation has been linked to several chronic inflammatory skin diseases and systemic sclerosis (18). In our study, AKT was expressed in the basal keratinocytes of the majority of LS samples, and less in control samples. AKT has previously been shown to be overexpressed in SSc fibroblasts and can also be activated by TGF-β and SMAD3 (23, 24), both of which were overexpressed in LS skin samples in our study. PI3K/AKT pathway thereby could be a promising treatment target in skin fibrosis.

Vactosertib and galunisertib, TGF-β receptor type I inhibitors, showed a strong decreasing trend in α-SMA and collagen-1 expression in LS fibroblasts in our

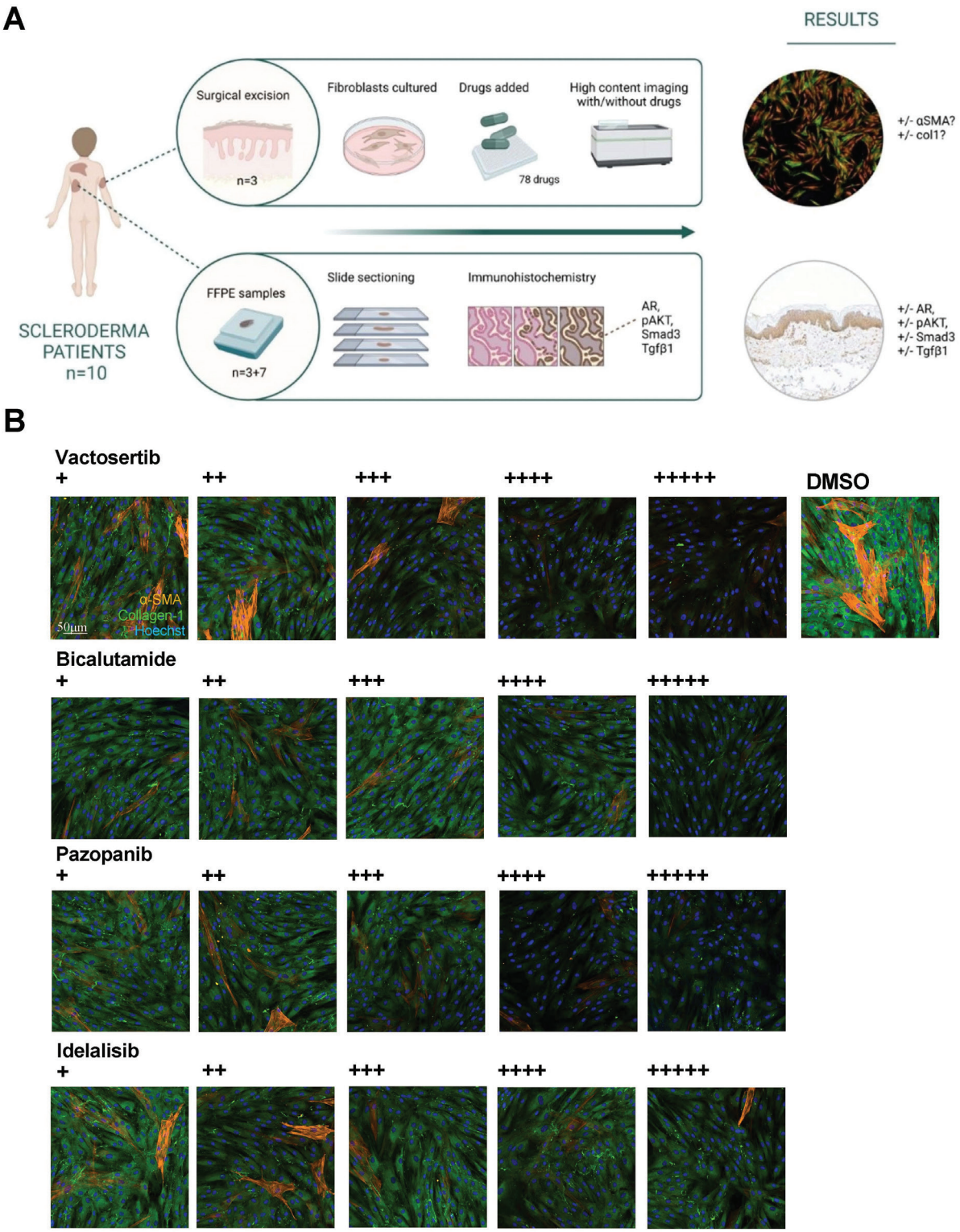

Fig. 1. (A) Study pipeline. Lesional skin biopsies were obtained from 10 localized scleroderma (LS) patients. Fibroblasts isolated from 3 biopsies were incubated with 78 drugs and stained with α-smooth muscle actin (α-SMA) and collagen-1. High content images were captured and analysed for antifibrotic effect. Immunohistochemistry was performed with FFPE skin biopsies using antibodies against phosphorylated AKT, transforming growth factor β1 (TGF-β1), SMAD3, and androgen receptor (AR). (B) Representative fluorescence microscopy images of drug-treated and untreated LS fibroblasts (LS patient 2). Fluorescence images showing expression of collagen-1 (green, 488 channel) and α-SMA (orange, 568 channel). Nuclei stained with Hoechst (blue, 408 channel). Images display LS fibroblasts for selected drugs and 0.1% DMSO (untreated), highlighting changes in marker expression and cell morphology. Expression of collagen-1 and α-SMA diminishes with increasing drug concentration. In untreated LS fibroblasts expression is abundant. Scale bar 50 μm.

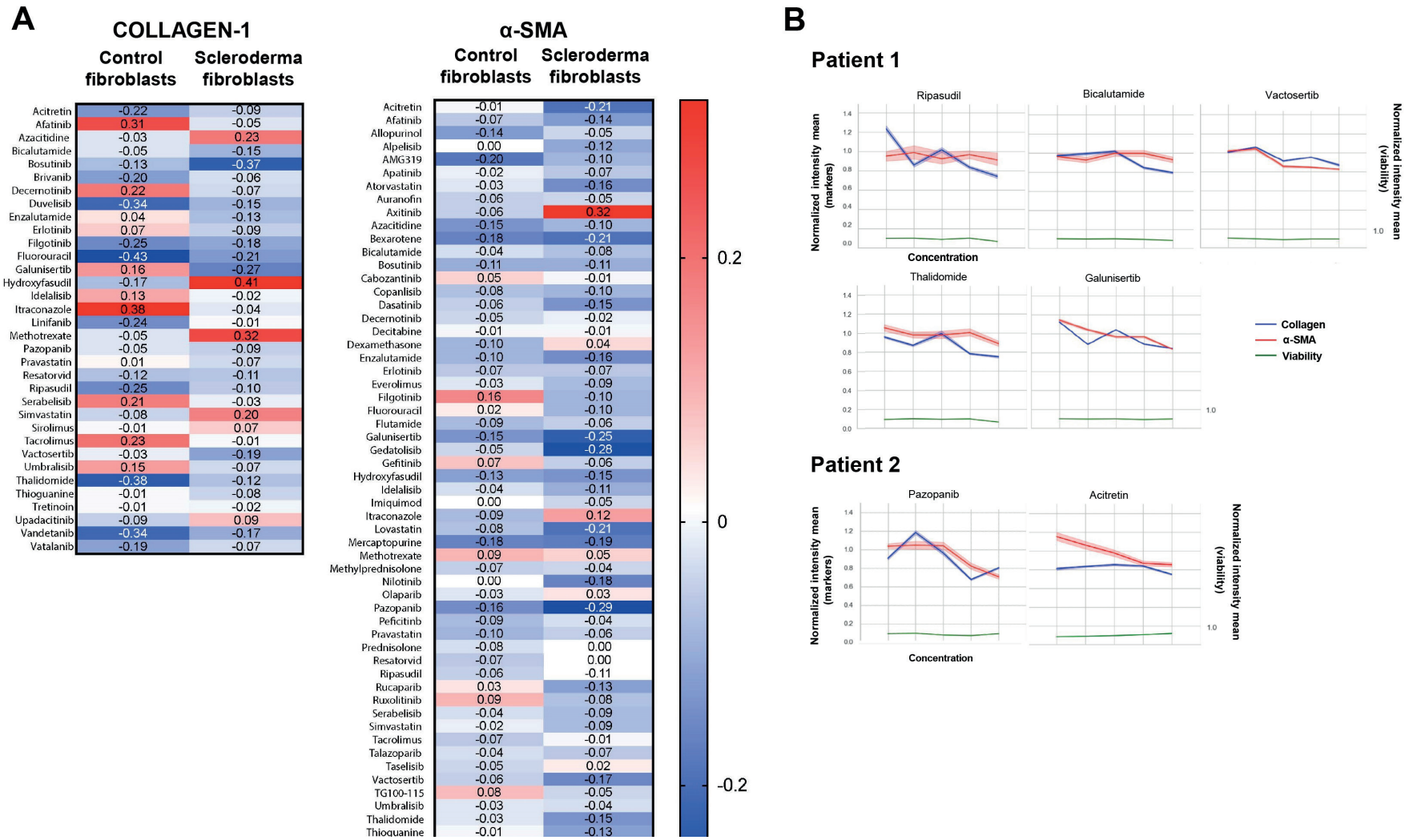

Fig. 2. Spearman correlation analysis of drug effects on collagen-1 and α-smooth muscle actin (α-SMA) expression (localized scleroderma [LS] patients 1 and 2). (A) Heatmaps showing Spearman correlation coefficients for collagen-1 and α-SMA, mean intensity values across increasing drug concentrations in LS and control fibroblasts. Negative correlations (blue) indicate a decreasing trend in marker expression with increasing drug concentrations. (B) Line plots illustrate representative examples of drugs with significant antifibrotic effect, showing normalized mean intensity values of collagen-1, α-SMA, and cell number across drug concentrations (mean intensity values are normalized to DMSO-treated controls). Viability is measured as the total number of cells (detected and segmented with the nuclei Hoechst signal).

Table II. Drugs with a significant ($p < 0.05$) antifibrotic effect by Spearman correlation test in scleroderma and control fibroblasts

Drug class	Scleroderma fibroblasts	*p*-value (α-SMA, collagen-1)	Control fibroblasts	*p*-value (α-SMA, collagen-1)
TGF-β receptor blockers	Vactosertib*	1.45e-282, 0.00	Vactosertib*	3.04e-20, 6.82e-7
	Galunisertib	0.00, 0.00		
Rho kinase inhibitors	Ripasudil	7.37e-30, 1.01e-23	Ripasudil	9.84e-06, 1.44e-83
			Hydroxyfasudil	1.15e-92, 4.04e-157
Tyrosine kinase inhibitors	Pazopanib	3.35e-210, 3.25e-23	Pazopanib	5.88e-38, 8.10e-5
	Bosutinib	5.88e-29, 1.68e-303	Bosutinib	3.46e-15, 1.52e-18
	Erlotinib	1.28e-39, 7.81e-68		
	Afatinib	3.95e-160, 1.37e-23		
	Vatalanib*	3.25e-5, 1.65e-14		
PI3k inhibitors	Idelalisib	1.05e-34, 6.95e-3		
	Serabelisib*	5.49e-72, 1.42e-10		
	Umbralisib	6.12e-16, 4.27e-49		
Androgen receptor blockers	Bicalutamide	1.49e-19, 2.21e-62	Bicalutamide	1.55e-3, 1.47e-4
	Enzalutamide	1.61e-76, 3.98e-47		
JAK inhibitors	Filgotinib (JAK1)	1.91e-89, 0.00		
	Decernotinib* (JAK3)	9.00e-6, 7.61e-41		
Statins	Pravastatin	2.15e-35, 4.14e-58		
Antimetabolites	Thioguanine	1.21e-46, 1.64e-14		
	Fluorouracil	2.02e-28, 9.85e-114		
Pyrimidine nucleoside analogues			Azacitidine	5.01e-31, 1.91e-2
Toll-like receptor blockers			Resatorvid*	5.97e-26, 7.93e-84
Retinoids	Acitretin	1.58e-125, 2.53e-25		
Other immunomodulatory drugs	Thalidomide	7.95e-62, 8.70e-39	Thalidomide	4.23e-2, 4.45e-192

*Investigational agent. TGF-β: transforming growth factor β; α-SMA: α-smooth muscle actin.

study. Vactosertib has been shown to have antifibrotic properties in hepatic, renal, pulmonary, and ulcerative colitis associated fibrosis in rat and mouse models by inhibiting the TGF-β/SMAD signalling pathway (25–27). Vactosertib has also been shown to inhibit fibrosis and increase lymphangiogenesis in a mouse tail model of acquired lymphoedema, and to reduce formation on post-surgical adhesion bands by inhibition of inflammation and fibrosis in mice (28, 29). The antifibrotic effect of vactosertib was seen here both in LS and control fibroblasts, whereas galunisertib affected specifically scleroderma fibroblasts. Galunisertib has been studied in TGF-β induced dermal fibroblasts, with decreasing effects on fibroblast proliferation and attenuation of fibrotic gene expression (30).

Rho-kinase has been linked to the pathogenesis of SSc and contributes to fibrosis through promoting myofibroblast differentiation and TGF-β signalling (31). Ripasudil and hydroxyfasudil had an antifibrotic effect in our study, confirming Rho-kinase inhibitors as potential antifibrotic treatments.

A novel finding in our study was the antifibrotic effect of AR antagonists bicalutamide and enzalutamide. The role of ARs in skin fibrosis is not well studied, and AR antagonists have not been investigated as potential treatments for either SSc or LS. Androgen receptors have, however, been linked to cardiac and ovarian fibrosis. The overexpression of ARs has been shown to increase TGF-β induced cardiac fibroblast proliferation and collagen production in mice, and a degradation enhancer of ARs attenuated cardiac fibrosis (32). In polycystic ovary syndrome transcriptional activation of androgen receptors via TGF-β signalling promoted ovarian fibrosis (33). Under normal conditions, ARs are expressed in the keratinocytes and dermal fibroblasts (34). In our study, AR expression was stronger in the keratinocytes of LS samples compared with controls, and it was also found in inflammatory cells. In mice, AR deficiency has been shown to significantly decrease the amount of collagen in tissues, indicating that blocking the receptor would lead to diminished collagen production (35).

In our study, significant antifibrotic effects were seen with filgotinib and decernotinib, but not with other tested JAK inhibitors. A JAK/STAT signalling cascade has been shown to be activated by TGF-β in dermal fibroblasts and JAK inhibition has been shown to diminish dermal fibrosis in SSc mouse models (36). Case reports of treatment of SSc and LS patients with JAK inhibitors (mostly tofacinitib and baricitinib) have been promising, with favourable effects on skin thickness (36).

There is evidence from past decades that retinoids affect the production of collagen from SSc fibroblasts, but clinical studies are few and they have scarcely been used in clinical practice in recent years (37). Retinoids have been more actively studied in renal, cardiac, and pulmonary fibrosis with positive effects (38–40). In our study, acitretin had a significant antifibrotic effect. As retinoids are commonly used by dermatologists to treat other conditions and have a favourable side effect profile compared with anti-cancer drugs, they could provide a possible treatment option for LS.

In conclusion, our study shows how LS patient fibroblasts can be utilized to screen shared and personalized drug responses. Our results indicate that PI3K/AKT and TGF-β pathway drugs have antifibrotic effects in LS fibroblasts, with AR blockers rising as potential novel therapies. As our patient cohort was small, further studies on the mechanisms and effects of these drugs in skin fibrosis and localized scleroderma are needed.

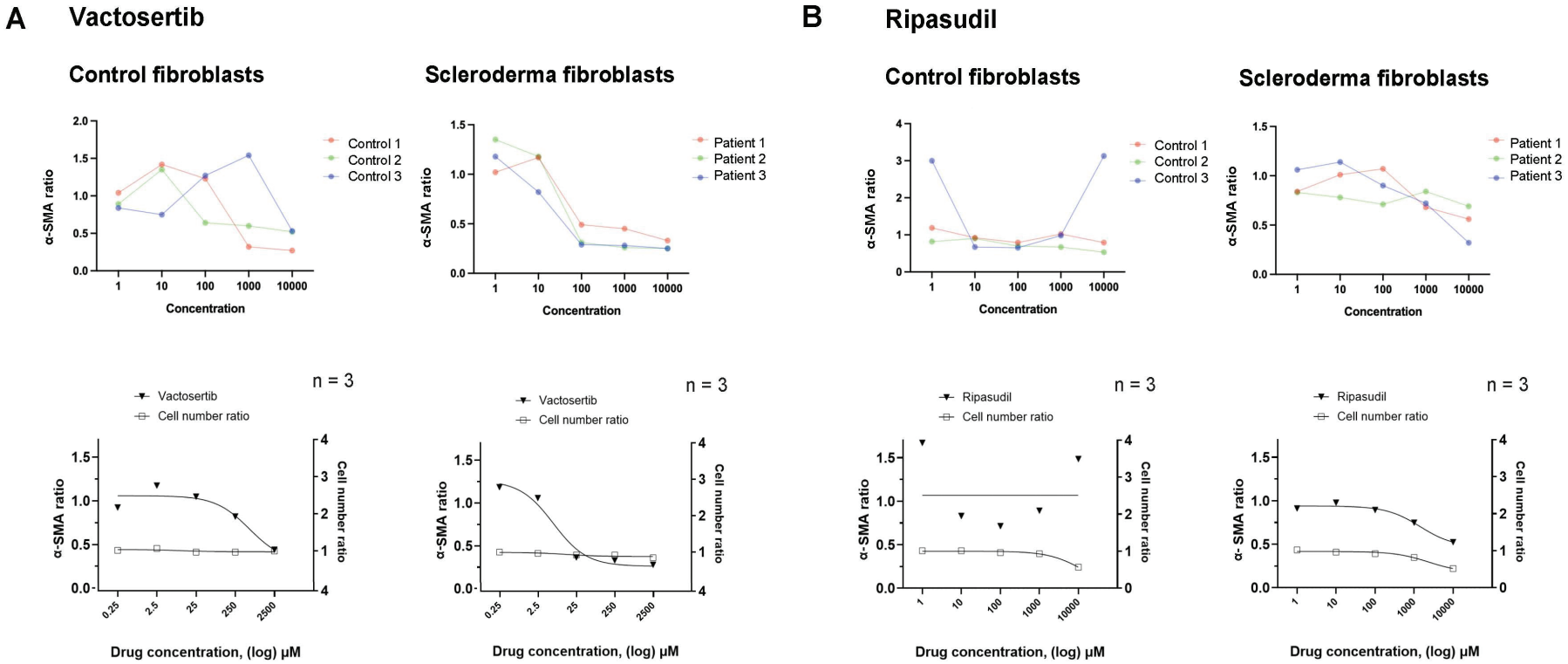

Fig. 3. Effect of selected drugs on α-smooth muscle actin (α-SMA)-positive cell ratio and total cell number. Curves represent α-SMA positive cell ratio relative to total cell number in localized scleroderma (LS) and control fibroblast, showing the effect of (A) vactosertib and (B) ripasudil. Upper curves show fibroblasts of individual LS patients and healthy controls, lower curves all controls and patients ($n = 3+3$). Cell number ratio indicates total number of cells (detected by Hoechst-stained nuclei) normalized with the average total cell number in untreated (DMSO) cells.

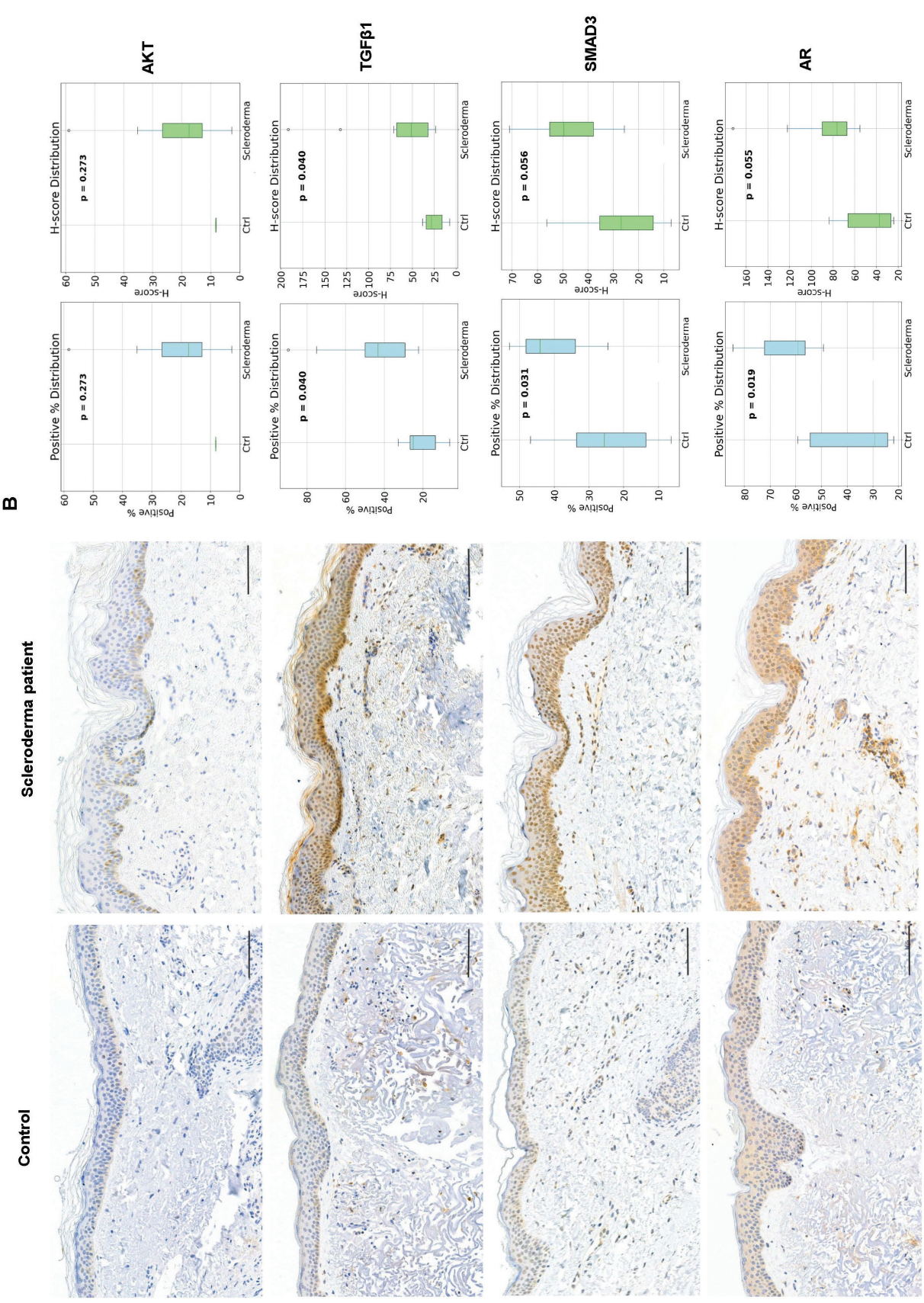

Fig. 4. (A) Representative immunostaining images of localized scleroderma (LS) and control skin FFPE tissue samples, stained with antibodies against phosphorylated AKT, androgen receptor (AR), SMAD3, and transforming growth factor β (TGF-β). AKT image is from LS patient 5, AR from patient 9, and TGF-β1 and SMAD3 from patient 10. Scale bar 100 µm. (B) Analysis of the percentage of positive cells of all the cells in epidermis and upper dermis and H-score in LS samples and healthy control skin.

ACKNOWLEDGEMENTS

The authors would like to commemorate professor Annamari Ranki and thank her for the initial inspiration and design of this project. Her collaboration and scientific capabilities are greatly valued.

Funding sources: This study has been supported by Finska Läkaresällskapet and Helsinki University Hospital Research Funds. The FIMM High Throughput Biomedicine Unit (EU-Openscreen) and the High Content Imaging and Analysis Unit (EuroBioImaging) are financially supported by the University of Helsinki (HiLIFE) and Biocenter Finland.

IRB approval status: This study has been approved by HUS ethical review board (HUS/16919/2022).

The authors have no conflicts of interest to declare.

REFERENCES

1. Fett N, Werth VP. Update on morphea: part I. Epidemiology, clinical presentation, and pathogenesis. J Am Acad Dermatol 2011; 64: 217–228; quiz 229–230. https://doi.org/10.1016/j.jaad.2010.05.045
2. Wenzel D, Haddadi NS, Afshari K, Richmond JM, Rashighi M. Upcoming treatments for morphea. Immun Inflamm Dis 2021; 9: 1101–1145. https://doi.org/10.1002/iid3.475
3. Kreuter A. Localized scleroderma. Dermatol Ther 2012; 25: 135–147. https://doi.org/10.1111/j.1529-8019.2012.01479.x
4. Saracino AM, Denton CP, Orteu CH. The molecular pathogenesis of morphoea: from genetics to future treatment targets. Br J Dermatol 2017; 177: 34–46. https://doi.org/10.1111/bjd.15001
5. Gilbane AJ, Denton CP, Holmes AM. Scleroderma pathogenesis: a pivotal role for fibroblasts as effector cells. Arthritis Res Ther 2013; 15: 215. https://doi.org/10.1186/ar4230
6. Abraham DJ, Eckes B, Rajkumar V, Krieg T. New developments in fibroblast and myofibroblast biology: implications for fibrosis and scleroderma. Curr Rheumatol Rep 2007; 9: 136–143. https://doi.org/10.1007/s11926-007-0008-z
7. van Caam A, Vonk M, van den Hoogen F, van Lent P, van der Kraan P. Unraveling SSc pathophysiology; the myofibroblast. Front Immunol 2018; 9: 2452. https://doi.org/10.3389/fimmu.2018.02452
8. Schulz JN, Plomann M, Sengle G, Gullberg D, Krieg T, Eckes B. New developments on skin fibrosis: essential signals emanating from the extracellular matrix for the control of myofibroblasts. Matrix Biol 2018; 68–69: 522–532. https://doi.org/10.1016/j.matbio.2018.01.025
9. Frangogiannis N. Transforming growth factor-beta in tissue fibrosis. J Exp Med 2020; 217: e20190103. https://doi.org/10.1084/jem.20190103
10. Knobler R, Geroldinger-Simic M, Kreuter A, Hunzelmann N, Moinzadeh P, Rongioletti F, et al. Consensus statement on the diagnosis and treatment of sclerosing diseases of the skin, Part 1: Localized scleroderma, systemic sclerosis and overlap syndromes. J Eur Acad Dermatol Venereol 2024; 38: 1251–1280. https://doi.org/10.1111/jdv.19912
11. Cronstein BN, Aune TM. Methotrexate and its mechanisms of action in inflammatory arthritis. Nat Rev Rheumatol 2020; 16: 145–154. https://doi.org/10.1038/s41584-020-0373-9
12. Bukiri H, Volkmann ER. Current advances in the treatment of systemic sclerosis. Curr Opin Pharmacol 2022; 64: 102211. https://doi.org/10.1016/j.coph.2022.102211
13. Henderson NC, Rieder F, Wynn TA. Fibrosis: from mechanisms to medicines. Nature 2020; 587: 555–566. https://doi.org/10.1038/s41586-020-2938-9
14. Blay V, Tolani B, Ho SP, Arkin MR. High-throughput screening: today's biochemical and cell-based approaches. Drug Discov Today 2020; 25: 1807–1821. https://doi.org/10.1016/j.drudis.2020.07.024
15. Khedoe P, Marges E, Hiemstra P, Ninaber M, Geelhoed M. Interstitial lung disease in patients with systemic sclerosis: toward personalized-medicine-based prediction and drug screening models of systemic sclerosis-related interstitial lung disease (SSc-ILD). Front Immunol 2020; 11: 1990. https://doi.org/10.3389/fimmu.2020.01990
16. Komura K, Yanaba K, Bouaziz JD, Yoshizaki A, Hasegawa M, Varga J, et al. Perspective to precision medicine in scleroderma. Front Immunol 2023; 14: 1298665. https://doi.org/10.3389/fimmu.2023.1298665
17. Kim Y, Nam Y, Rim YA, Ju JH. Anti-fibrotic effect of a selective estrogen receptor modulator in systemic sclerosis. Stem Cell Res Ther 2022; 13: 303. https://doi.org/10.1186/s13287-022-02987-w
18. Roy T, Boateng ST, Uddin MB, Banang-Mbeumi S, Yadav RK, Bock CR, et al. The PI3K-Akt-mTOR and associated signaling pathways as molecular drivers of immune-mediated inflammatory skin diseases: update on therapeutic strategy using natural and synthetic compounds. Cells 2023; 12: 1671. https://doi.org/10.3390/cells12121671
19. Qian Y, Peng K, Qiu C, Skibba M, Huang Y, Xu Z, et al. Novel epidermal growth factor receptor inhibitor attenuates angiotensin II-induced kidney fibrosis. J Pharmacol Exp Ther 2016; 356: 32–42. https://doi.org/10.1124/jpet.115.228080
20. Wei X, Han J, Chen ZZ, Qi BW, Wang GC, Ma YH, et al. A phosphoinositide 3-kinase-gamma inhibitor, AS605240 prevents bleomycin-induced pulmonary fibrosis in rats. Biochem Biophys Res Commun 2010; 397: 311–317. https://doi.org/10.1016/j.bbrc.2010.05.109
21. Russo RC, Garcia CC, Barcelos LS, Rachid MA, Guabiraba R, Roffe E, et al. Phosphoinositide 3-kinase gamma plays a critical role in bleomycin-induced pulmonary inflammation and fibrosis in mice. J Leukoc Biol 2011; 89: 269–282. https://doi.org/10.1189/jlb.0610346
22. Maher TM, Strek ME. Antifibrotic therapy for idiopathic pulmonary fibrosis: time to treat. Respir Res 2019; 20: 205. https://doi.org/10.1186/s12931-019-1161-4
23. Jun JB, Kuechle M, Min J, Shim SC, Kim G, Montenegro V, et al. Scleroderma fibroblasts demonstrate enhanced activation of Akt (protein kinase B) in situ. J Invest Dermatol 2005; 124: 298–303. https://doi.org/10.1111/j.0022-202X.2004.23559.x
24. Suwanabol PA, Seedial SM, Zhang F, Shi X, Si Y, Liu B, et al. TGF-beta and Smad3 modulate PI3K/Akt signaling pathway in vascular smooth muscle cells. Am J Physiol Heart Circ Physiol 2012; 302: H2211–2219. https://doi.org/10.1152/ajpheart.00966.2011
25. Park SA, Kim MJ, Park SY, Kim JS, Lee SJ, Woo HA, et al. EW-7197 inhibits hepatic, renal, and pulmonary fibrosis by blocking TGF-beta/Smad and ROS signaling. Cell Mol Life Sci 2015; 72: 2023–2039. https://doi.org/10.1007/s00018-014-1798-6
26. Kim MJ, Park SA, Kim CH, Park SY, Kim JS, Kim DK, et al. TGF-beta type I receptor kinase inhibitor EW-7197 suppresses cholestatic liver fibrosis by inhibiting HIF1alpha-induced epithelial mesenchymal transition. Cell Physiol Biochem 2016; 38: 571–588. https://doi.org/10.1159/000438651
27. Binabaj MM, Asgharzadeh F, Avan A, Rahmani F, Soleimani A, Parizadeh MR, et al. EW-7197 prevents ulcerative colitis-associated fibrosis and inflammation. J Cell Physiol 2019; 234: 11654–11661. https://doi.org/10.1002/jcp.27823
28. Yoon SH, Kim KY, Wang Z, Park JH, Bae SM, Kim SY, et al. EW-7197, a transforming growth factor-beta type I receptor kinase inhibitor, ameliorates acquired lymphedema in a mouse tail model. Lymphat Res Biol 2020; 18: 433–438. https://doi.org/10.1089/lrb.2018.0070
29. Soleimani A, Asgharzadeh F, Rahmani F, Avan A, Mehraban S, Fakhraei M, et al. Novel oral transforming growth factor-beta signaling inhibitor potently inhibits postsurgical adhesion band formation. J Cell Physiol 2020; 235: 1349–1357. https://doi.org/10.1002/jcp.29053
30. Peterson JM, Jay JW, Wang Y, Joglar AA, Prasai A, Palackic A, et al. Galunisertib exerts antifibrotic effects on TGF-beta-induced fibroproliferative dermal fibroblasts. Int J Mol Sci

2022; 23: 6689. https://doi.org/10.3390/ijms23126689
31. Zanin-Zhorov A, Blazar BR. ROCK2, a critical regulator of immune modulation and fibrosis has emerged as a therapeutic target in chronic graft-versus-host disease. Clin Immunol 2021; 230: 108823. https://doi.org/10.1016/j.clim.2021.108823
32. Wang Y, Ma W, Lu S, Yan L, Hu F, Wang Z, et al. Androgen receptor regulates cardiac fibrosis in mice with experimental autoimmune myocarditis by increasing microRNA-125b expression. Biochem Biophys Res Commun 2018; 506: 130–136. https://doi.org/10.1016/j.bbrc.2018.09.092
33. Wang D, Zhu Z, Fu Y, Zhang Q, Zhang Y, Wang T, et al. Bromodomain-containing protein 4 activates androgen receptor transcription and promotes ovarian fibrosis in PCOS. Cell Rep 2023; 42: 113090. https://doi.org/10.1016/j.celrep.2023.113090
34. Ceruti JM, Leiros GJ, Balana ME. Androgens and androgen receptor action in skin and hair follicles. Mol Cell Endocrinol 2018; 465: 122–133. https://doi.org/10.1016/j.mce.2017.09.009
35. Markova MS, Zeskand J, McEntee B, Rothstein J, Jimenez SA, Siracusa LD. A role for the androgen receptor in collagen content of the skin. J Invest Dermatol 2004; 123: 1052–1056. https://doi.org/10.1111/j.0022-202X.2004.23494.x
36. McGaugh S, Kallis P, De Benedetto A, Thomas RM. Janus kinase inhibitors for treatment of morphea and systemic sclerosis: a literature review. Dermatol Ther 2022; 35: e15437. https://doi.org/10.1111/dth.15437
37. Thomas RM, Worswick S, Aleshin M. Retinoic acid for treatment of systemic sclerosis and morphea: a literature review. Dermatol Ther 2017; 30. https://doi.org/10.1111/dth.12455
38. Watanabe H, Bi J, Murata R, Fujimura R, Nishida K, Imafuku T, et al. A synthetic retinoic acid receptor agonist Am80 ameliorates renal fibrosis via inducing the production of alpha-1-acid glycoprotein. Sci Rep 2020; 10: 11424. https://doi.org/10.1038/s41598-020-68337-z
39. Leem AY, Shin MH, Douglas IS, Song JH, Chung KS, Kim EY, et al. All-trans retinoic acid attenuates bleomycin-induced pulmonary fibrosis via downregulating EphA2-EphrinA1 signaling. Biochem Biophys Res Commun 2017; 491: 721–726. https://doi.org/10.1016/j.bbrc.2017.07.122
40. Lin XY, Chu Y, Zhang GS, Zhang HL, Kang K, Wu MX, et al. Retinoid X receptor agonists alleviate fibroblast activation and post-infarction cardiac remodeling via inhibition of TGF-beta1/Smad pathway. Life Sci 2023; 329: 121936. https://doi.org/10.1016/j.lfs.2023.121936